Stochastic and deterministic phase slippage in quasi-one-dimensional superconducting nanowires exposed to microwaves

2012 New J. Phys. 14 043014

(http://iopscience.iop.org/1367-2630/14/4/043014)

New Journal of Physics
The open-access journal for physics

Stochastic and deterministic phase slippage in quasi-one-dimensional superconducting nanowires exposed to microwaves

Myung-Ho Bae[1,2,3], **R C Dinsmore III**[1], **M Sahu**[1] **and A Bezryadin**[1]

[1] Department of Physics, University of Illinois at Urbana-Champaign, Urbana, IL 61801-3080, USA

[2] Division of Convergence Technology, Korea Research Institute of Standards and Science, Daejeon 305-340, Korea

E-mail: mhbae@kriss.re.kr

New Journal of Physics **14** (2012) 043014 (15pp)
Received 18 August 2011
Published 17 April 2012
Online at http://www.njp.org/
doi:10.1088/1367-2630/14/4/043014

Abstract. We study current–voltage (V–I) characteristics of short superconducting nanowires of length ~ 100 nm exposed to microwave (MW) radiation of frequencies between 2 and 15 GHz. The radiation causes a decrease of the average switching current of the wire. This suppression of the switching current is modeled assuming that there is one-to-one correspondence between Little's phase slips, which are microscopic stochastic events induced by thermal and quantum fluctuations, and the experimentally observed switching events. We also find that at some critical power P^* of the radiation a dissipative dynamic superconducting state occurs as an extra step on the V–I curve. It is identified as a phase slip center (PSC), which is essentially a deterministic and periodic in-time phase rotation. With the dependence of the switching currents and the standard deviations observed at the transitions: (i) from the supercurrent state to the normal state and (ii) from the supercurrent state to the PSC regime, we conclude that both of the two types of switching events are triggered by the same microscopic event, namely a single-phase slip. We show that the Skocpol–Beasley–Tinkham model is not applicable to our MW-driven PSCs, probably due to the tendency of the PSC to synchronize with the MW. Through the analysis of the switching current distributions at a sufficiently low temperature, we also present evidence that quantum phase slips play a role in switching events even under MWs.

[3] Author to whom any correspondence should be addressed.

Contents

1. Introduction

Fluctuations, both thermal and quantum, play an important role in determining the physical properties of one-dimensional (1D) superconducting systems. These fluctuations cause the occurrence of events, such as Little's phase slips (LPSs), in which the phase difference between the ends of the wire (i.e. the phase of the superconducting order parameter) 'slips' by 2π [1]. Under constant supercurrent the order parameter takes the shape of a spiral in the Argand diagram, extended with one more axis representing the position along the wire. Each LPS causes this spiral to lose or gain one turn. The LPS can only happen if the order parameter goes to zero at one point on the wire. Note that the number of turns multiplied by 2π gives the total phase difference between the ends of the wire. At high temperatures, thermal activation of LPSs is the dominant mechanism and is well understood both experimentally and theoretically ([2, 3] and references therein). At sufficiently low temperatures, quantum phase slips (QPS) are possible [4]. The QPS in nanowires, which is an example of macroscopic quantum tunneling, remains a topic of active research [5]. A novel type of evidence for the existence of QPS was recently obtained through the excessive switching current fluctuations at high bias currents [6]. In relation to nanowires, it has been suggested that superconducting nanowires can be used to build qubits [7, 8].

Here we study the general microwave (MW) response of superconducting nanowires. When an MW signal is applied to the wires and its power increased, we observe a reduction in the switching current, I_{SW}, followed by the appearance of a dynamical superconducting regime, i.e. a phase slip center (PSC). The existence of coherence in this regime is supported by the observation of Shapiro steps on the voltage–current (V–I) characteristics (figure 2(b)). The behaviors of I_{SW} of the wire and of the PSC under MW are studied in detail. It is concluded that the triggering mechanism for different types of switching events is the same. Namely, the switching from the constant supercurrent state to the PSC and the switching from the constant supercurrent state to the Joule normal state (JNS) are triggered by the same underlying microscopic fluctuation effect—the LPSs. This means that we rule out such a hypothetical situation that to start a PSC process a single LPS is needed, while to produce JNS a coincidence of many LPSs is needed. What we find is that a single LPS, if it happens, must switch the wire either to PSC or to JNS, depending on the bias current at sufficiently low temperatures. The

switching from PSC to JNS appears to have a different switching mechanism. We also provide evidence of QPS at low temperatures (~ 0.35 K), under MW radiation.

In previous studies, PSC have been observed in wires near the superconducting transition temperature, T_c, because the wires were rather thick due to technical limitations [9]. By increasing the temperature it was possible to achieve the 1D superconductivity regime since the coherence length ξ (which needs to be larger than the wire diameter in order to achieve the 1D regime) diverges near T_c. The main difference lies in the fact that our nanowires are extremely thin and remain quasi-1D down to zero temperature. Thus our type of wires opens up a possibility of studying the dynamics of the quasi-1D condensate, including PSCs, down to temperatures approaching absolute zero. On the other hand, in our type of suspended nanowires, Joule heating prevented us from observing PSC without MW being applied. Therefore, a study carried out under MW radiation is presented here. The purpose of this paper is to generalize the notion of PSC down to temperatures much smaller than the critical temperature. By PSC we understand a deterministic, dynamic, periodic in time, state of the condensate.

2. Fabrication and measurements

As shown in figure 1, we fabricate nanowire devices based on the molecular templating technique [2] that was originally described in [10] and further improved in [11]. With this technique it was, in the past, possible to make superconducting or insulating single nanowire devices [10] as well as single superconducting wire resonators and devices with multiple wires in parallel [12]. The fabrication is achieved by placing a fluorinated single-carbon nanotube over a trench in the substrate and then sputter-coating the nanotube with the desired superconducting material. A ~ 100 nm wide and ~ 5 mm long trench is prepared on a 60 nm thick SiN film on 500 μm thick SiO_2/Si wafer by electron beam lithography and the reactive ion etching process. To define an undercut in the exposed SiO_2 layer through the trench, the SiO_2 is etched in a $\sim 50\%$ concentrated HF-in-water solution. This undercut ensures electrical disconnection between electrodes across the trench except through the suspended nanowire. To form the wire, fluorinated carbon nanotubes are distributed on the substrate from a solution in isopropyl alcohol. After blowing the solution with a nitrogen gas, a desired superconducting metal is deposited by dc magnetron sputtering. Here 5–15 nm of $Mo_{79}Ge_{21}$ (MoGe) is deposited on the suspended nanotubes to form the nanowires. During this process, the metal covers the top of the nanotubes.

Figure 1(b) shows a scanning electron microscope (SEM) image of a typical suspended nanotube that is coated with MoGe. The beginning and the end of the suspended nanotube show white regions, the so-called 'white spots', indicated by arrows. These white spots appear in the SEM images because the nanotube is suspended over the tilted side of the trench (see figure 1(a)). They indicate that the nanowire is straight, which is important to exclude the possibility of the formation of a weak link in the superconducting nanowire. A transmission electron micrograph (TEM) image in figure 1(c) shows that such nanowires appear to be continuous and homogeneous. Some apparent surface roughness could originate from the amorphous morphology of the wire and the surface oxidation in air.

All the samples are wired in a four-probe configuration (figure 1(a), inset), with each twisted pair of voltage and current lines. The bias current is applied using a precision voltage function generator, Stanford Research Systems (SRS) DS360, connected in series with a standard resistor R_s. The R_s value is much larger than the sample resistance. The voltage across

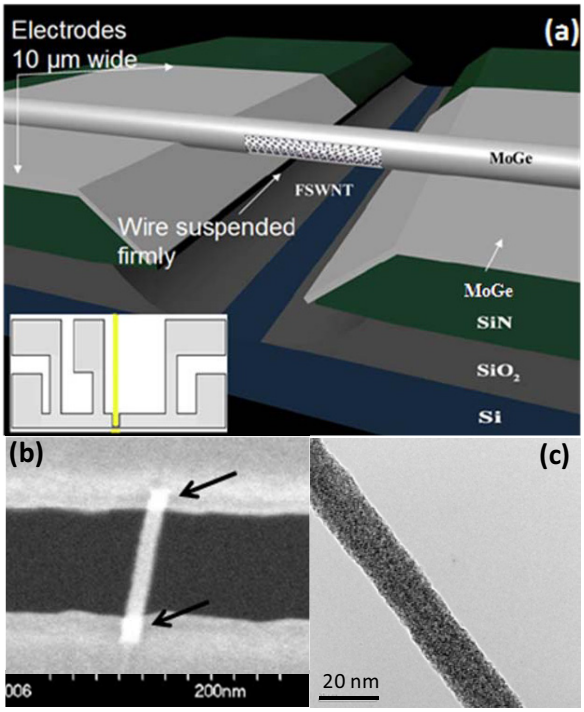

Figure 1. MoGe nanowire prepared by the molecular templating method. (a) Schematic representation of the molecular templating technique for the growth of nanometer-scale nanowires. Fluorinated single-wall carbon nanotubes are deposited across a trench defined on a substrate and are then sputter-coated with a layer of MoGe alloy 5–15 nm thick. Inset: schematic representation of the contact pads (gray) and the electrodes (gray) connected to the wire. The electrodes are made in the same sputtering run as the wire itself. The yellow line in the inset shows the trench over which the templating nanotube is positioned. (b) SEM images of a nanowire. The brighter spots (shown by arrows) near the banks of the trench indicate that the wire is suspended straightly and firmly across the gap. (c) A TEM of typical MoGe nanowires.

the standard resistor and the voltage across the sample are amplified using either the SR530 or the PAR 113 preamplifier. The preamplifiers are battery-powered and thus have a low noise level at the input terminals. The outputs of these preamps are fed to an analogue–digital convertor board. The temperature is measured using a ruthenium oxide thermometer that is wired in a four-probe configuration and measured using the Lakeshore 370A temperature controller. To achieve the desired temperature, the output current of the temperature controller is applied to either a heater attached to the 3He pot or the sorption pump heaters. Using this system, we are able to maintain temperatures within approximately 5 mK or better. The MW signal is generated by a Gigatronics 1026 function generator, which can output signals from −99 to +10 dBm for frequencies in the range 1 MHz–26 GHz. The signal is capacitively (and inductively) coupled to the sample through an antenna positioned at the bottom of the sample Faraday cage. Because of the cage, we were only able to study the sample's response at resonant frequencies of the cage.

3. Results and discussion

3.1. Microwave (MW) response of superconducting nanowires

Figure 2(a) shows *V–I* curves of the nanowires at various temperatures, which show a hysteretic behavior below $T = 2.9$ K. At $T = 358$ mK, as bias current is swept from zero to higher values, the wire switches (the switching appears as a large voltage jump on the *V–I* curve) from a superconducting state (SCS) to a resistive or normal state. The switching can be caused by LPSs and then by Joule heating [13]. It was found previously that the switching is triggered by each single LPS at sufficiently low temperatures, while at higher temperatures (empirically, higher than $\sim$1 K) a temporal approximate coincidence of a few LPSs is needed to overheat the wire and produce the switching [6, 14]. The corresponding switching current I_{SW} is stochastic, meaning that at each time that the *V–I* curve is measured one obtains a slightly different value for I_{SW}. Once in the normal state, the *V–I* curve is linear with the slope almost exactly equal to the normal resistance of the entire wire. The normal state is marked 'JNS' in figure 2(a). In the inset of figure 2(b), the JNS is also visible at the highest current bias shown in the plot. The signature of the JNS is the resistance being equal to the normal state resistance. When the bias current is decreased considerably below I_{SW}, the wire jumps back to the SCS at the retrapping current I_R (see the lower inset of figure 2(a)). The SCS is the state in which the voltage on the wire is zero although the current is not zero. This I_R is not stochastic, meaning that in every measurement the same value of I_R (with the precision of the setup) is observed (also see figure 3(b)). This deterministic nature indicates that the resistive state is simply a normal state, stabilized due to Joule heating of the wire [15]. In this case the retrapping is explained by the cooling of the wire below its T_c as the bias current is decreased. Since the cooling process involves a macroscopic number of degrees of freedom, associated with normal electrons, the fluctuation of the I_R is not observed (the relative value of fluctuations is proportional to $1/\sqrt{N}$, where N is the number of degrees of freedom involved).

Increasing the temperature from 358 mK suppresses I_{SW} while the retrapping current remains constant up to $T \sim 2.5\,\text{K} < T_c$ (see figure 3(a)). At intermediate temperatures $2.5\,\text{K} < T < 3.1\,\text{K}$, both I_{SW} and I_R are suppressed with increasing temperature and there is a finite voltage due to thermally activated LPSs which appears as 'resistive tails' in the *V–I* curves, before the switching occurs [6] (e.g. see curve 5 in the lower inset of figure 2(a)). This fact represents an important piece of evidence that at high enough temperatures single LPSs can occur in the wire without necessarily causing the switching into JNS. In other words, many LPSs need to occur almost simultaneously to generate enough heat to switch the wire into JNS. Such a multiple LPS process is well described by the models developed recently by Shah *et al* [14]. The same model and the absence of resistive tails at low temperatures (roughly below 1 K) indicate that at low temperatures each single LPS causes the observable switch, either into the JNS (or into the PSC state if MWs are applied) [6, 14]. As the temperature increases from $T = 3.1$ K to $T = T_c$ ($= 4.1$ K), the hysteresis disappears and I_{SW} goes to zero.

Figure 2(b) shows the MW response (for frequency $f = 7.34$ GHz) on *V–I* curves at $T = 350$ mK. The MW response of the wire shows some similarity to the temperature response in figure 2(a) but it is different enough to rule out the trivial heating of the nanowire with the MW radiation. When the power of the MW signal increases from zero, I_{SW} of the wire decreases and I_R does not change. In that respect the effect of MW is similar to the effect of heating.

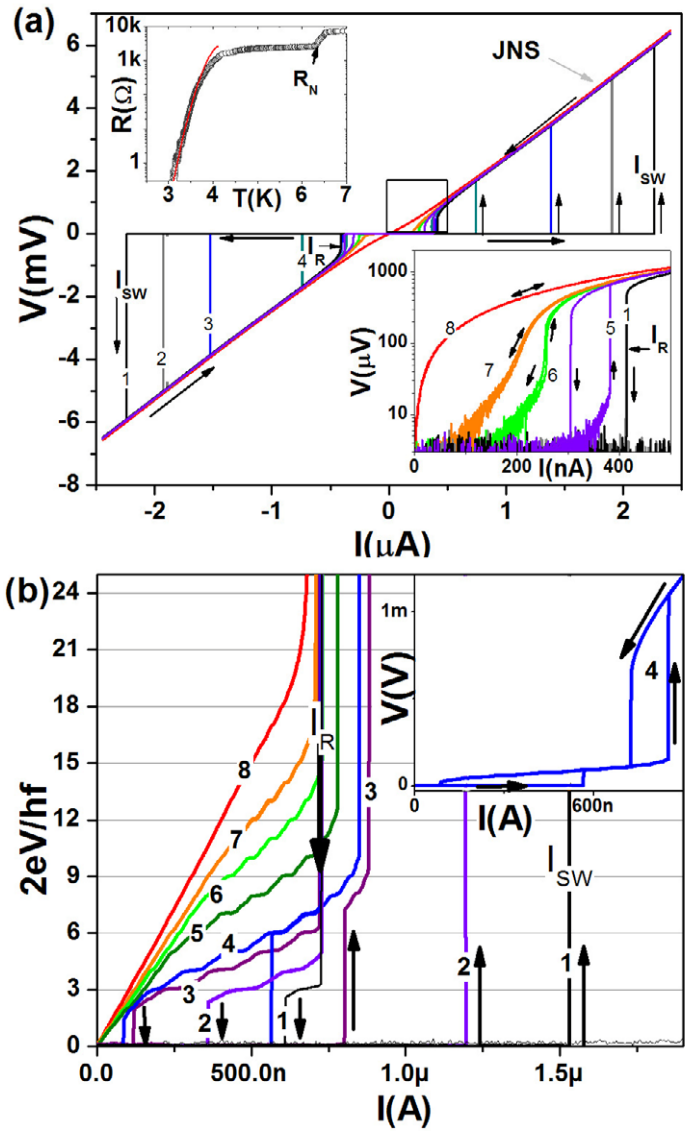

Figure 2. (a) V–I characteristics for the sample 121707C numbered according to increasing temperature (no MW signal is applied here): (1) $T = 358$ mK, (2) $T = 1$ K, (3) $T = 1.8$ K, (4) $T = 2.5$ K, (5) $T = 2.9$ K, (6) $T = 3.1$ K, (7) $T = 3.4$ K and (8) $T = 4.1$ K, above T_c of the wire. The critical currents I_{SW} and I_R are indicated. After the switching at I_{SW} the wire reaches the normal state resistance. Lower inset: log scale of the boxed region with curves 2–4 removed for clarity. Curves 6–8 are measured at higher temperatures, at which the switching events are smeared due to thermal fluctuations. Upper inset: R versus T for the sample with fit to the TAPS theory with parameters $R_N = 2760\,\Omega$, $T_c = 4.1$ K, $L = 110$ nm and $\xi(0) = 10.2$ nm. The resistance drop at 6.5 K is due to the leads going superconducting. The normal resistance of the wire R_N is taken to be the value measured right below the temperature at which leads become superconducting. This value is indicated by the arrow. (b) Positive bias V–I characteristics for the sample 121707C as the MW signal

Figure 2. (Continued) of various powers is applied. The frequency is $f = 7.34$ GHz and the temperature is $T = 350$ mK. The voltage drop on the wire is normalized by the radiation photon energy, as indicated (here $\hbar$ is Planck's constant, e is the electron charge and f is the frequency). Shapiro steps are clearly observed at integer values of the normalized voltage. The curves are numbered according to increasing MW power, P, measured at the source output, in dBm: (1) −5.1, (2) −4.7, (3) −4.2, (4) −3.4, (5) −2.5, (6) −1, (7) 0.2 and (8) 2. Inset: the general view of the V–I curve under MWs. The formation of a PSC, assisted by the applied MW radiation, is observed at low bias as a resistive state with the resistance much lower than the normal resistance.

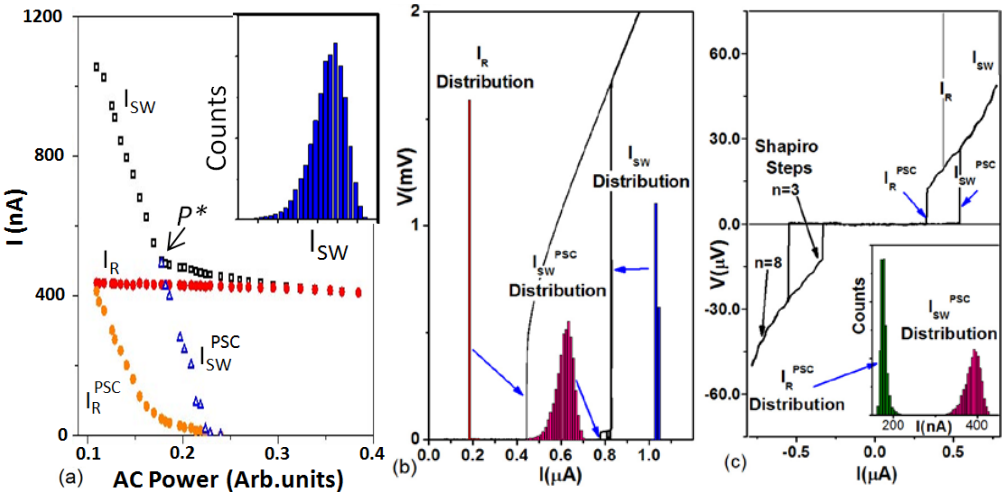

Figure 3. (a) Switching and retrapping currents versus MW power at 3 GHz for the sample 121707C. The switching current I_{SW} (I_{SW}^{PSC}) corresponds to the switching into the normal (phase-slip) state, and retrapping from the normal (phase-slip) state, I_R (I_R^{PSC}). The power P^*, indicated above, is defined as the power when a PSC first appears in the switching branch (inset of figure 2(b)). The power P^* also corresponds to the kink in the curve. Inset: a representative histogram for I_{SW} at power $P < P^*$. (b) Positive bias segment of a V–I curve for ten traces for a power just above P^*. The histograms shown are for counts of a given I_R, I_{SW} and I_{SW}^{PSC}. The jumps whose statistics is measured are indicated by the blue arrows. The probability distributions are computed from 10 000 total scans. The distributions are scaled to fit the figure. Only the switching current from the SCS to the PSC (I_{SW}^{PSC}) shows a broad distribution. (c) V–I curve at $P > P^*$ and at a bias slightly below I_{SW}. Shapiro steps are visible with steps corresponding to $V = nhf/2e$ with $n = 3$ and $n = 8$ indicated by arrows. Inset: distributions for the switching current, I_{SW}^{PSC}, and the retrapping current, I_R^{PSC}, for the PSC for 10 000 scans. Both critical currents for the PSC are stochastic. All data shown here were measured at a temperature of 500 mK.

At higher powers of applied MW, an additional resistive branch occurs in the V–I curve (see the inset of figure 2(b)), either before the switching to the normal state (as the current is swept up, so the corresponding branch is called the sweeping-up branch) or after the retrapping from

the normal state (as the current is swept down, corresponding to the sweeping-down branch). The occurrence of the branch takes place at a certain power, P^* of MW, in the sweeping-up branch, and at P^R in the sweeping-down branch of the *V–I* curve.

We interpret this new resistive branch (which is not observed if the temperature is increased and no MW is applied) as an MW-assisted PSC. This observation broadens the options of investigating the dynamics of the order parameter in nanowires since without the radiation it is impossible to observe a PSC, since the wire always overheats and jumps into the JNS near I_{SW}. When the MWs are applied, our results are analogous to the observations of Anderson and Dayem, performed on rather wide superconducting bridges [16]. The effects of increasing MW power on I_{SW} and I_R are better summarized in figure 3. As the MW power increases from 0 to P^*, I_{SW} for the SCS $\rightarrow$ JNS transition monotonically decreases while remaining stochastic and the JNS $\rightarrow$ SCS transition at I_R remains constant and deterministic. Figure 3(a) shows this trend by plotting I_{SW} and I_R as a function of MW power. The kink in the plot is indicative of the onset of a PSC branch in the sweeping-up branch, which occurs at $P = P^*$.

For powers higher than P^* two jumps in the *V–I* curve are observed when the current is increased: the first jump represents SCS $\rightarrow$ PSC and the second jump corresponds to PSC $\rightarrow$ JNS (figure 2(b), inset). Thus, for $P > P^*$, we introduce two notations for the jumps: I_{SW}^{PSC} representing the transition SCS $\rightarrow$ PSC and I_{SW} representing the transition PSC $\rightarrow$ JNS. Histograms in figure 3(b) show that while the transition SCS $\rightarrow$ PSC remains highly stochastic, the transition PSC $\rightarrow$ JNS exhibits a very narrow, almost deterministic distribution. When the current is reduced we also observe either one or two retrapping events. The retrapping current for the transition *from the normal branch* to either the fully superconducting branch or the PSC state is denoted by I_R. The retrapping current for the transition from the PSC branch to the fully superconducting branch is denoted by I_R^{PSC}. The PSC is a dynamic SCS as evidenced by the appearance of Shapiro steps and the stochastic nature of both the switching current (I_{SW}^{PSC}) and the retrapping current (I_R^{PSC}) (see figure 3(c)). Unlike the SCS $\leftrightarrow$ JNS transition, the SCS $\leftrightarrow$ PSC transition is clearly stochastic in both directions.

The transition SCS $\rightarrow$ PSC follows the same trend as the transition SCS $\rightarrow$ JNS at powers lower than P^*, in the sense that (a) the width of the distribution of I_{SW} for $P < P^*$ is very similar to the width of the distribution of I_{SW}^{PSC} at $P > P^*$, and (b) the slope of I_{SW} versus P for $P < P^*$ is very similar to the slope of the curve I_{SW}^{PSC} versus P at $P > P^*$ (see figure 3(a)). These observations strongly indicate that the same physics for the transition out of the SCS to the JNS for $P < P^*$ and out of the SCS to the PSC for $P > P^*$ is involved. The Shapiro steps occur due to synchronization of the superconducting phase difference rotation with the applied high-frequency MW radiation and were discussed in detail in [17]. The steps appear at voltage values given by $2\,\mathrm{eV} = nhf$, as expected, where e is the elementary charge, n is an integer number and $\hbar$ is the Plank constant. Shapiro steps are only present in the portion of the *V–I* curve attributed to the PSC. The lack of the Shapiro step in the high-voltage regime (i.e. the JNS regime) independently verifies that this regime is indeed a non-coherent (i.e. normal) state.

3.2. MW-induced phase slip centers and the Skocpol–Beasley–Tinkham model

Our quasi-1D wires are too narrow to support a normal vortex core even at zero temperature, thus enabling us to study PSC down to temperatures much lower than the critical temperature. In the Skocpol, Beasley and Tinkham (SBT) model of the PSC [18], the order parameter is suppressed in a small region of the wire that is of the order of 2ξ in length.

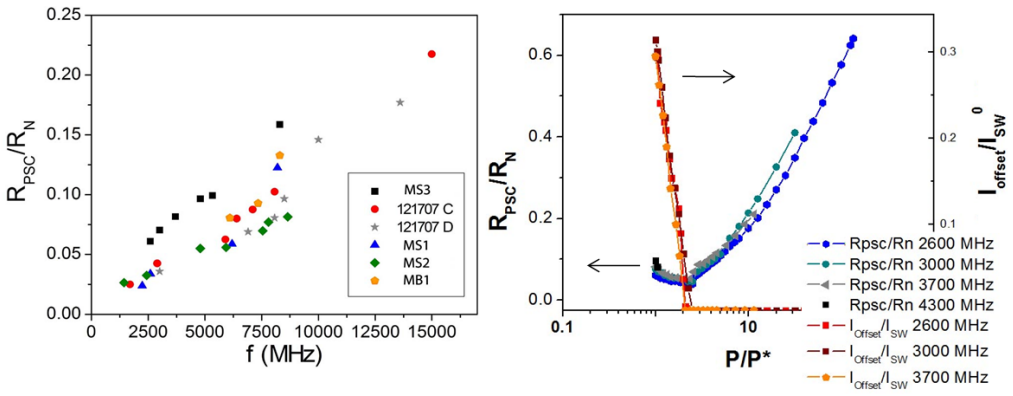

Figure 4. (a) Average resistance (normalized by R_N) versus frequency for six samples taken at ~ 350 mK and MW power slightly greater than P^*. The data show that the average resistance of the MW-assisted PSC monotonically increases with the frequency of the applied MW. (b) R_{PSC}/R_N and I_{offset}/I_{SW} versus P/P^* for three frequencies for the sample MS3. Resistance is taken as a linear fit of the first few steps in the V–I characteristic. A kink in R_{PSC} occurs near where the offset current goes to zero.

The generated Bogoliubov quasi-particles [2] then diffuse a distance Λ_Q (quasi-particle diffusion length), typically much longer than ξ, away from the center of the PSC before relaxing back into the condensate. This model predicts that the voltage of the PSC will be given by $V = 2\rho\Lambda_Q(I - \beta I_S)/A$ with I being the dc bias current, I_S the supercurrent, A the cross-sectional area of the wire, ρ the resistivity of the wire material (for the used MoGe alloy $\rho \sim 200\,\mu\Omega$ cm) and β a constant of the order of $\frac{1}{2}$ such that βI_S is the time-averaged supercurrent flowing through the PSC. This model predicts the differential resistance of the PSC to be given by $R_{PSC} = 2\rho\Lambda_Q/A$ or equivalently $R_{PSC}/R_N = 2\Lambda_Q/L$ with R_N and L being, correspondingly, the normal state resistance and the length of the nanowire. The differential resistance we measure in MW-assisted PSC depends strongly on the MW frequency and ranges from nearly zero to 1 kΩ at radiation powers slightly above P^*. Figure 4(a) is a plot of R_{PSC}/R_N versus f for six different samples. Note that according to the SBT model, if applied to our observations, the ratio R_{PSC}/R_N should be equal to the length of the dissipative region (which is the length over which the quasi-particles propagate before relaxing into the condensate) of the PSC divided by the total length of the wire. That the length of our nanowires is about 100 nm and the coherence length ξ is about 10 nm. So, according to SBT, the minimum expected value for the ratio $R_{PSC}/R_N = 2\Lambda_Q/L$ is 0.2, because the quasi-particles should at least exist within the core, which cannot be smaller than the coherence length. Still smaller values have been observed, as low as 0.025 for this ratio (figure 4(a)). Here, the average resistance of the PSC (R_{PSC}) was taken by a linear fit of the V–I curve, in the range $I_{SW}^{PSC} < I < I_{SW}$. The observed very low values of this ratio, suggesting according to the SBT model that the core is smaller than the coherence length in some cases, appear to be unphysical. Thus, we conclude that the SBT model is not applicable to the PSC under investigation, which exists at low temperatures compared to T_c and the MW radiation. Hopefully future theoretical work will lead to an appropriate generalization of the SBT model to describe MW-assisted PSCs, described in this work.

Figure 4(b) shows measurements of R_{PSC}/R_N and the normalized offset current, I_{offset}/I_{SW}, for the sample MS3 as a function of applied MW power at three different frequencies. The offset current is the current when an extrapolated line from a PSC branch meets the current axis. It is interesting to note that the resistance of the PSC measured in this manner decreases slightly with increasing power and then exhibits a small discontinuous jump, and as the power increases further, the PSC resistance also increases. On the other hand, the offset current, which within the SBT model represents the time average of the supercurrent, decreases steadily to zero when the MW power is increased.

The presence of the PSC branch can be explained as follows: if the system jumps to the PSC state at a low enough bias current, then Joule heating is weak enough so that the wire does not jump to the JNS immediately, but only when the current is further increased to generate strong-enough heating (at which point the second jump, now to the normal state, is observed). The offset current for the PSC decreases with increasing MW power, so a low-resistance PSC will appear first (as the MW power is increased) in the current-sweeping-up branch at P^* and then in the current-sweeping-down branch when the offset current is decreased below I_R. This explanation is based on the observation that the PSC cannot exist at currents lower than the offset current. For powers below but near P^* the intersection of the PSC branch with the overheating transition occurs at a very high voltage and the power dissipated in the wire is high enough to heat the wire above T_c. Thus, when the wire switches into the PSC branch it immediately goes normal because the wire cannot dissipate the heat generated by the bias current. In this case the PSC only appears in the retrapping branch (see curves 1 and 2 in figure 2(b)). A PSC that appears first in the current-sweeping-down branch will appear in the current-sweeping-up branch at a slightly higher MW power. At higher power the switching current, I_{SW}, is further reduced and intersects the PSC branch at a lower voltage. This voltage is low enough that the Joule heating is not sufficient to heat the wire above T_c. At powers in this regime a stable dynamic SCS exists and the system stays in the PSC branch until the current is increased to I_{SW}.

3.3. Switching current distributions and quantum phase slips

Before discussing the behavior of the switching event in a wire exposed to MW radiation, we will first review the recent results on this process in the purely dc case without MW [6, 14]. In [6], the authors studied the stochastic nature of the switching current at different temperatures to understand the underlying mechanism that leads to the transition from the SCS to the JNS. What they found was that the distribution of switching currents became broader as the temperature was lowered. This rather counter-intuitive trend is due to a crossover of the multiple LPS switching mechanism to a single-LPS switching mechanism with lowering temperature. In order to understand quantitatively the occurrence of the switching events and their relationship with LPSs, they consider the thermal conductivity of the superconducting nanowire system [14]. The wire is a suspended structure measured in a vacuum. So the heat dissipated in the wire must be conducted to the leads where it can be dissipated further. Joule heat is generated when an LPS occurs. When this happens a small region of the wire becomes heated and possibly normal. Thus, it will generate more heat, due to the Joule heating effect, since the wire is biased with a constant current. The amount of heat dissipated by each LPS is $Ih/2e$ [14], where I is the bias current. Using this relationship and a numerical model for thermal conductivity it was shown that at temperatures lower than approximately 1 K a single LPS is sufficient to cause the wire to overheat and switch from the SCS to the JNS. Qualitatively speaking, this is because at low

temperatures the fluctuations are weak and so the phase slips can occur only very near I_c, where the barrier for phase slips is strongly suppressed. At the same time, at bias currents close to I_c, the temperature needs to increase only slightly in order to become larger than the current-dependent critical temperature. That is why a single phase slip taking place at bias currents close to I_c is always able to overheat the wire.

To determine whether this single LPS is due to thermal or quantum fluctuations the switching current distribution (SCD) can be converted into a switching rate using the Kurkijarvi method [19], which was generalized and extensively used to analyze switching events in current-biased Josephson junctions by Fulton and Dunkleberger in [20] (the model is developed for the cases when the bias, which reduces the barrier for the switching, is increased linearly in time). The measured rates, Γ, are then compared to the rates for the two types of LPS processes, namely thermally activated phase slips (TAPS), which are described by the Langer–Ambegaokar–McCumber–Halperin (LAMH) model [1], and phenomenological QPS (Giordano model) [4, 21]:

$$\Gamma_{\mathrm{TAPS}} = \Omega_{\mathrm{TAPS}} \exp\left(-\frac{\Delta F(T, I)}{k_{\mathrm{B}} T}\right)$$
$$= \left(\frac{L}{\xi(T)}\right)\left(\frac{1}{\tau_{\mathrm{GL}}}\right)\left(\frac{\Delta F(T)}{k_{\mathrm{B}} T}\right)^{1/2} \exp\left(-\frac{\Delta F(T, I)}{k_{\mathrm{B}} T}\right), \tag{1a}$$

$$\Gamma_{\mathrm{QPS}} = \Omega_{\mathrm{QPS}} \exp\left(-\frac{\Delta F(T, I)}{k_{\mathrm{B}} T_{\mathrm{QPS}}}\right)$$
$$= \left(\frac{L}{\xi(T)}\right)\left(\frac{1}{\tau_{\mathrm{GL}}}\right)\left(\frac{\Delta F(T)}{k_{\mathrm{B}} T_{\mathrm{QPS}}}\right)^{1/2} \exp\left(-\frac{\Delta F(T, I)}{k_{\mathrm{B}} T_{\mathrm{QPS}}}\right). \tag{1b}$$

Here $\tau_{\mathrm{GL}} = [\pi\hbar/8k_{\mathrm{B}}(T_c - T)]$ is the Ginzburg–Landau relaxation time, Ω is the attempt rate and T_{QPS} is the temperature-dependent effective temperature for a QPS from the Giordano model, having the free energy barrier given by [14, 22]

$$\Delta F(T, I) = \frac{\sqrt{6}\hbar I_c(T)}{2e}\left(1 - \frac{I}{I_c}\right)^{5/4}. \tag{2}$$

The results in [6] corresponding to low temperatures (0.3–1 K) were in good agreement with Giordano's model of QPS and were not consistent with the TAPS model. Thus, switching event statistics at low temperatures of $T = 0.3$ K is used to obtain evidence for QPS in the following section.

3.4. The effect of MWs on the switching current distribution

We have already discussed how MWs can lead to the suppression of the switching current, but now we will discuss how they affect the SCD. Figure 5 shows SCDs and the corresponding switching rates versus the bias current for the sample 091608B for increasing applied MW power from −99 to −34 dBm. The data are taken with a 5 Hz sweep rate and 10 000 points for each distribution. The rates (figure 5, bottom panel) are fitted to the single QPS model using the procedure outlined above. According to the overheating model as introduced in the previous section [13], it turns out that this wire is in the single QPS regime at temperatures lower than

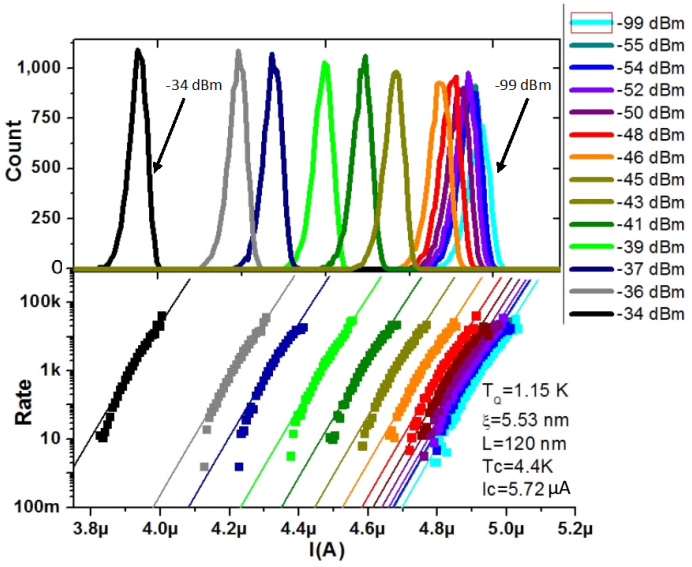

Figure 5. SCDs and rates at different MW powers, taken at $T = 300$ mK for the sample 091608B. Top: 10 000 point SCDs taken at the MW powers given in the legend. Bottom: rates for the SCDs in the top graph along with fits to the single QPS model. The fitting parameters are shown in the lower legend and are close to the values used in the overheating model. The values for $I_{\mathrm{RF}}^{\mathrm{Fit}}$ (and only this parameter was changed) were changed to fit each curve. The resulting values of the fitting parameter are shown in figure 6.

about 1.15 K. In this regime a single phase slip (either thermal or quantum) is always sufficient to cause the wire to switch from an SCS to the JNS state. In this case, the rate of QPS is equal to the experimentally measured switching rate, so equation (1*b*) can be applied. However, we need to incorporate the effect of the applied MW radiation into this model.

When we expose the wire to the MW radiation, we introduce an ac bias to the wire in addition to the dc bias. In this case, we can compute the free energy barrier for an LPS to occur using the following equation:

$$\Delta F(T, I) = \frac{\sqrt{6}\hbar I_{\mathrm{c}}(T)}{2e}\left(1 - \frac{I_{\mathrm{DC}} + I_{\mathrm{RF}}\sin\omega t}{I_{\mathrm{c}}}\right)^{5/4}, \tag{3}$$

where I_{DC} is the dc bias current and I_{RF} is the amplitude of the ac bias current with angular frequency, ω, induced in the wire from the MW antenna and t is the time. Using equations (1*b*) and 3, we can compute the switching rate for a single QPS event. To do this we first perform average of the rate over one period of the MW signal, to get the time-averaged switching rate. This procedure is justified because the setup used to measure the switching rate is much slower than the frequency of the applied MW. Using this strategy we can compute the switching rate as a function of temperature, dc bias current, $I_{\mathrm{c}}(T)$, ξ, T_{c}, T_{QPS} and the ac bias current I_{RF} and use this computed curve to fit the experimental data. The parameters ξ and T_{c} are taken to be the values obtained using TAPS fits and T_{QPS} and $I_{\mathrm{c}}(T)$ are determined by the overheating model for temperature dependence of the switching current. These parameters may be changed slightly from those values. However, we assume that they remain fixed for all rates at different

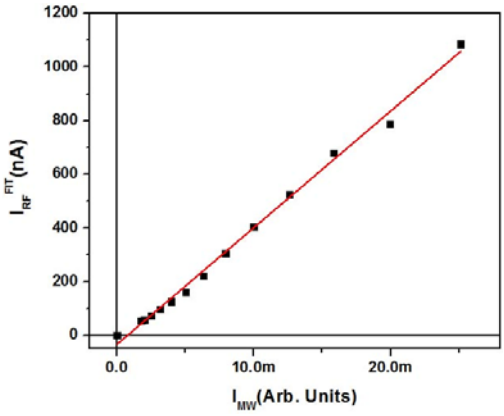

Figure 6. Fitting parameters, $I_{\mathrm{RF}}^{\mathrm{Fit}}$, versus applied MW current for the sample 091608B. The other parameters used are those given in figure 5. The line is the best linear fit to the data points.

MW powers. Thus, the only parameter to fit the rates measured at various applied MW powers is $I_{\mathrm{RF}}^{\mathrm{Fit}}$. SCDs are measured for one wire at a constant temperature at several MW powers, as shown in the upper panel of figure 5. The rates are then computed using the above procedure and they are fitted using this model by varying $I_{\mathrm{RF}}^{\mathrm{Fit}}$ (see the lower panel of figure 5). The absolute value of the experimental MW-induced amplitude I_{MW} is not known; however, it must be proportional to the square root of the applied MW power. This applied ac bias current, I_{MW}, in arbitrary units, is computed from the applied MW power as $I_{\mathrm{MW}} = (10^{P/10})^{1/2}$, where P is the power in dBm. If the I_{RF} obtained by this model is proportional to I_{MW}, then the model is consistent with the experiment. It is important to note that this simple model is not expected to work for values of I_{RF} that approach the critical current closely. The results of the fitting procedure for the values of $I_{\mathrm{RF}}^{\mathrm{Fit}}$ are plotted as a function of the applied dimensionless MW current, I_{MW}, in figure 6.

The linear fit in figure 6 is rather good, indicating that the proposed interpretation based on the assumption that, at low temperatures, single QPS events trigger observable jumps on the V–I curve (the SCS $\rightarrow$ PSC switch, to be more precise) under MW irradiation is valid.

4. Conclusions

The physical properties of MW-induced and MW-sustained PSCs were examined in detail. We show that the PSCs observed in the *suspended* superconducting nanowires under MWs do not behave like those studied near T_{c} in previous experiments. The switching transitions SCS $\rightarrow$ JNS (superconductor $\rightarrow$ normal), occurring at zero or low powers, were compared with the switching transitions of the type SCS $\rightarrow$ PSC (superconductor to PSC) at sufficiently high MW powers. We present strong evidence that each of those transitions is caused by the same triggering mechanism. Namely, at sufficiently low temperatures, a single phase slippage by 2π (which is termed LPS) is always sufficient to switch the wire, either to a normal state or to a resistive state with a PSC. Further, we compare the results with the Giordano model for the QPS rate, extended to include an MW radiation condition. It is argued that single QPSs represent the main cause for the switching events at low temperatures, even under MWs.

Acknowledgments

This paper is based upon work supported by the US Department of Energy's Division of Materials Sciences under award no. DE-FG02-07ER46453 through the Frederick Seitz Materials Research Laboratory, University of Illinois at Urbana-Champaign. The present work was also supported by NSF grant no. DMR 10-05645. Part of this work was carried out in the Frederick Seitz Materials Research Laboratory Central Facilities, University of Illinois.

References

[1] Little W A 1967 Decay of persistent currents in small superconductors *Phys. Rev.* **156** 396–403
Langer J S and Ambegaokar V 1967 Intrinsic resistive transition in narrow superconducting channels *Phys. Rev.* **164** 498–510
McCumber D E and Halperin B I 1970 Time scale of intrinsic resistive fluctuations in thin superconducting wires *Phys. Rev.* B **1** 1054–70
McCumber D E 1968 Intrinsic resistive transition in thin superconducting wires driven from current sources *Phys. Rev.* **172** 427–9
[2] Tinkham M 1996 *Introduction to Superconductivity* 2nd edn (New York: McGraw-Hill)
[3] Bezryadin A 2008 Quantum suppression of superconductivity in nanowires *J. Phys.: Condens. Matter* **20** 043202
[4] Giordano N 1988 Evidence for macroscopic quantum tunneling in one-dimensional superconductors *Phys. Rev. Lett.* **61** 2137–40
[5] Zaikin A D, Golubev D S, Otterlo A V and Zimanyi G T 1997 Quantum phase slips and transport in ultrathin superconducting wires *Phys. Rev. Lett.* **78** 1552–5
Zgirski M, Riikonen K-P, Touboltsev V and Arutyunov K 2005 Size dependent breakdown of superconductivity in ultranarrow nanowires *Nano Lett.* **5** 1029–33
Meidan D, Oreg Y and Refael G 2007 Sharp superconductor–insulator transition in short wires *Phys. Rev. Lett.* **98** 187001
Zgirski M, Riikonen K-P, Touboltsev V and Arutyunov K Yu 2008 quantum fluctuations in ultranarrow superconducting aluminum nanowires *Phys. Rev.* B **77** 054508
Khlebnikov S 2008 Quantum phase slips in a confined geometry *Phys. Rev.* B **77** 014505
[6] Sahu M, Bae M-H, Rogachev A, Pekker D, Wei T-C, Shah N, Goldbart P M and Bezryadin A 2009 Individual topological tunnelling events of a quantum field probed through their macroscopic consequences *Nature Phys.* **5** 503
[7] Mooij J E and Harmans C J P M 2005 Phase-slip flux qubits *New J. Phys.* **7** 219
[8] Ku J, Manucharyan V and Bezryadin A 2010 Superconducting nanowires as nonlinear inductive elements for qubits *Phys. Rev.* B **82** 134518
[9] Lukens J E, Warburton R J and Webb W W 1970 Onset of quantized thermal fluctuations in 'one-dimensional' superconductors *Phys. Rev. Lett.* **25** 1180–84
Newbower R S, Beasley M R and Tinkham M 1972 Fluctuation effects on the superconducting transition of tin whisker crystals *Phys. Rev.* B **5** 864–8
Tidecks R and Meyer J D 1979 Current-induced resistive state of superconducting tin whiskers with indium impurities *Z. Phys.* B **32** 363–74
[10] Bezryadin A, Lau C N and Tinkham M 2000 Quantum suppression of superconductivity in ultrathin nanowires *Nature* **404** 971–4
[11] Bollinger A T, Dinsmore III R C, Rogachev A and Bezryadin A 2008 Determination of the superconductor–insulator phase diagram for one-dimensional wires *Phys. Rev. Lett.* **101** 227003
[12] Brenner M W, Gopalakrishnan S, Ku J, McArdle T J, Eckstein J N, Shah N, Goldbart P M and Bezryadin A 2011 Crated Lorentzian response of driven microwave superconducting nanowire-bridged resonators: oscillatory and magnetic-field induced stochastic states *Phys. Rev.* B **83** 184503

Belkin A, Brenner M, Aref T, Ku J and Bezryadin A 2011 Little–Parks oscillations at low temperatures: Gigahertz resonator method *Appl. Phys. Lett.* **98** 242504

[13] Kramer L and Baratoff A 1977 Lossless and dissipative current-carrying states in quasi-one-dimensional superconductors *Phys. Rev. Lett.* **38** 518–21

Kramer L and Watts-Tobin R J 1978 Theory of dissipative current-carrying states in superconducting filaments *Phys. Rev. Lett.* **40** 1041–44

Watts-Tobin R J, Krahenbuhl Y and Kramer L 1981 Nonequilibrium theory of dirty, current-carrying superconductors: phase-slip oscillators in narrow filaments near Tc *J. Low Temp. Phys.* **42** 459–501

Kramer L and Rangel R 1984 Structure and properties of the dissipative phase-slip state in narrow superconducting filaments with and without inhomogeneities *J. Low Temp. Phys.* **57** 391–414

[14] Shah N, Pekker D and Goldbart P M 2008 Inherent stochasticity of superconductor–resistor switching behavior in nanowires *Phys. Rev. Lett.* **101** 207001

Pekker D, Shah N, Sahu M, Bezryadin A and Goldbart P M 2009 Stochastic dynamics of phase-slip trains and superconductive-resistive switching in current-biased nanowires *Phys. Rev.* B **80** 214525

[15] Tinkham M, Free J U, Lau C N and Markovic N 2003 Hysteretic *I–V* curves of superconducting nanowires *Phys. Rev.* B **68** 134515

[16] Anderson P W and Dayem A H 1964 Radio-frequency effects in superconducting thin film bridges *Phys. Rev. Lett.* **13** 195–7

[17] Dinsmore III R C, Bae M-H and Bezryadin A 2008 Fractional order Shapiro steps in superconducting nanowires *Appl. Phys. Lett.* **93** 192505

Bae M-H, Dinsmore III R C, Aref T, Brenner M and Bezryadin A 2009 Current-phase relationship, thermal and quantum phase slips in superconducting nanowires made on a scaffold created using adhesive tape *Nano Lett.* **9** 1889–96

[18] Skocpol W J, Beasley M R and Tinkham M 1974 Phase-slip centers and nonequilibrium processes in superconducting tin microbridges *J. Low Temp. Phys.* **16** 145–67

[19] Kurkijarvi J 1972 Intrinsic fluctuations in a superconducting ring closed with a Josephson junction *Phys. Rev.* B **6** 832–5

[20] Fulton T A and Dunkleberger L N 1974 Lifetime of the zero-voltage state in Josephson tunnel junctions *Phys. Rev.* B **9** 4760–8

[21] Lau C N, Markovic N, Bockrath M, Bezryadin A and Tinkham M 2001 Quantum phase slips in superconducting nanowires *Phys. Rev. Lett.* **87** 217003

[22] Tinkham M and Lau C N 2002 Quantum limit to phase coherence in thin superconducting wires *Appl. Phys. Lett.* **80** 2946